



---

Year: 2021

---

## Regional brain mGlu5 receptor occupancy following single oral doses of mavoglurant as measured by [11C]-ABP688 PET imaging in healthy volunteers

Streffer, Johannes ; Treyer, Valerie ; Buck, Alfred ; Ametamey, Simon M ; Blagoev, Milen ; Maguire, Ralph P ; Gautier, Aurélie ; Auberson, Yves P ; Schmidt, Mark E ; Vranesic, Ivan-Toma ; Gomez-Mancilla, Baltazar ; Gasparini, Fabrizio

**Abstract:** Mavoglurant binds to same allosteric site on metabotropic glutamate receptor 5 (mGluR5) as [11C]-ABP688, a radioligand. This open-label, single-center pilot study estimates extent of occupancy of mGluR5 receptors following single oral doses of mavoglurant, using [11C]-ABP688 positron emission tomography (PET) imaging, in six healthy males aged 20–40 years. This study comprised three periods and six subjects were divided into two cohorts. On Day 1 (Period 1), baseline clinical data and safety samples were obtained along with PET scan. During Period 2 (1–7 days after Period 1), cohort 1 and 2 received mavoglurant 25 mg and 100 mg, respectively. During Period 3 (7 days after Period 2), cohort 1 and 2 received mavoglurant 200 mg and 400 mg, respectively. Mavoglurant showed the highest distribution volumes in the cingulate region with lower uptake in cerebellum and white matter, possibly because myelinated axonal sheets maybe devoid of mGlu5 receptors. Maximum concentrations of mavoglurant were observed around 2–3.25 h post-dose. Mavoglurant passed the blood–brain barrier and induced dose- and exposure-dependent displacement of [11C]-ABP688 from the mGluR5 receptors, 3–4 h post-administration (27%, 59%, 74%, 85% receptor occupancy for mavoglurant 25 mg, 100 mg, 200 mg, 400 mg dose, respectively). There were no severe adverse effects or clinically significant changes in safety parameters. This is the first human receptor occupancy study completed with Mavoglurant. It served to guide the dosing of mavoglurant in the past and currently ongoing clinical studies. Furthermore, it confirms the utility of [11C]-ABP688 as a unique tool to study drug-induced occupancy of mGlu5 receptors in the living human brain.

DOI: <https://doi.org/10.1016/j.neuroimage.2021.117785>

Posted at the Zurich Open Repository and Archive, University of Zurich

ZORA URL: <https://doi.org/10.5167/uzh-200716>

Journal Article

Published Version



The following work is licensed under a Creative Commons: Attribution-NonCommercial-NoDerivatives 4.0 International (CC BY-NC-ND 4.0) License.

Originally published at:

Streffer, Johannes; Treyer, Valerie; Buck, Alfred; Ametamey, Simon M; Blagoev, Milen; Maguire, Ralph P; Gautier, Aurélie; Auberson, Yves P; Schmidt, Mark E; Vranesic, Ivan-Toma; Gomez-Mancilla, Baltazar; Gasparini, Fabrizio (2021). Regional brain mGlu5 receptor occupancy following single oral doses of mavoglurant as measured by [11C]-ABP688 PET imaging in healthy volunteers. *NeuroImage*, 230:117785. DOI: <https://doi.org/10.1016/j.neuroimage.2021.117785>



## Regional brain mGlu5 receptor occupancy following single oral doses of mavoglurant as measured by [<sup>11</sup>C]-ABP688 PET imaging in healthy volunteers

Johannes Streffer<sup>a,1,2</sup>, Valerie Treyer<sup>b,3</sup>, Alfred Buck<sup>b</sup>, Simon M. Ametamey<sup>c</sup>, Milen Blagoev<sup>b</sup>, Ralph P Maguire<sup>d,1</sup>, Aurélie Gautier<sup>e</sup>, Yves P. Auberson<sup>d</sup>, Mark E. Schmidt<sup>d,4</sup>, Ivan-Toma Vranesic<sup>d,5</sup>, Baltazar Gomez-Mancilla<sup>d,6</sup>, Fabrizio Gasparini<sup>d,\*</sup>

<sup>a</sup> Division of Psychiatric Research, University of Zurich, Zurich, Switzerland

<sup>b</sup> Department of Nuclear Medicine, University Hospital Zurich, University of Zurich, Zurich, Switzerland

<sup>c</sup> Radiopharmaceutical Sciences, Institute of Pharmaceutical Sciences, Zurich, Switzerland

<sup>d</sup> Novartis Institutes for Biomedical Research, Novartis Pharma AG, Postfach, Basel CH-4002, Switzerland

<sup>e</sup> Global Drug Development, Novartis Pharma AG, Basel, Switzerland

### ARTICLE INFO

#### Keywords:

Mavoglurant

mGluR5

PET imaging

Receptor occupancy

Single oral dose

### ABSTRACT

Mavoglurant binds to same allosteric site on metabotropic glutamate receptor 5 (mGluR5) as [<sup>11</sup>C]-ABP688, a radioligand. This open-label, single-center pilot study estimates extent of occupancy of mGluR5 receptors following single oral doses of mavoglurant, using [<sup>11</sup>C]-ABP688 positron emission tomography (PET) imaging, in six healthy males aged 20–40 years. This study comprised three periods and six subjects were divided into two cohorts. On Day 1 (Period 1), baseline clinical data and safety samples were obtained along with PET scan. During Period 2 (1–7 days after Period 1), cohort 1 and 2 received mavoglurant 25 mg and 100 mg, respectively. During Period 3 (7 days after Period 2), cohort 1 and 2 received mavoglurant 200 mg and 400 mg, respectively. Mavoglurant showed the highest distribution volumes in the cingulate region with lower uptake in cerebellum and white matter, possibly because myelinated axonal sheets maybe devoid of mGlu5 receptors. Maximum concentrations of mavoglurant were observed around 2–3.25 h post-dose. Mavoglurant passed the blood–brain barrier and induced dose- and exposure-dependent displacement of [<sup>11</sup>C]-ABP688 from the mGluR5 receptors, 3–4 h post-administration (27%, 59%, 74%, 85% receptor occupancy for mavoglurant 25 mg, 100 mg, 200 mg, 400 mg dose, respectively). There were no severe adverse effects or clinically significant changes in safety parameters.

This is the first human receptor occupancy study completed with Mavoglurant. It served to guide the dosing of mavoglurant in the past and currently ongoing clinical studies. Furthermore, it confirms the utility of [<sup>11</sup>C]-ABP688 as a unique tool to study drug-induced occupancy of mGlu5 receptors in the living human brain.

### 1. Introduction

L-glutamate is a major excitatory neurotransmitter in the mammalian central nervous system. Glutamate signaling involves activation of a family of receptors including G-protein-coupled metabotropic receptors (mGluRs) and ionotropic glutamate receptors. mGluRs play

an important modulatory role in synaptic transmission, and are distributed in various regions of the brain (Vose and Stanton, 2017; Reiner and Levitz, 2018; Suh et al., 2018). The mGluR subtype 5 (mGluR5), with post-synaptic expression, is found in high abundance in the limbic brain areas including the hippocampus, forebrain, striatal regions, and amygdala (Swanson et al., 2005). These receptors are potentially important therapeutic targets for a number of neurological and therapeutic disorders including depression, fragile X syndrome (FXS),

\* Corresponding author.

E-mail address: [fabrizio.gasparini@novartis.com](mailto:fabrizio.gasparini@novartis.com) (F. Gasparini).

<sup>1</sup> UCB Early Solutions, UCB Biopharma SPRL, Braine-l'Alleud, Belgium.

<sup>2</sup> Reference Center for Biological Markers of Dementia (BIODEM), University of Antwerp, Antwerp, Belgium.

<sup>3</sup> Institute for Regenerative Medicine (IREM), University of Zurich, Zurich, Switzerland.

<sup>4</sup> Neuroscience Therapeutic Area, Janssen Research and Development, Division of Janssen Pharmaceutica, Beerse, Belgium 2340.

<sup>5</sup> Global Drug Development, Novartis Pharma AG, Basel, Switzerland.

<sup>6</sup> Department of Neurology and Neurosurgery, McGill University, Montréal, Canada.

anxiety, obsessive-compulsive disorders (OCD), and levodopa-induced dyskinesia in Parkinson's disease (PD-LID) (Dolen and Bear, 2008; Michalon et al., 2012; Akkus et al., 2014; Jaeschke et al., 2015). Additionally, mGluR5 antagonists have demonstrated anxiolytic actions in a variety of animal models, suggesting their potential to treat various anxiety disorders (panic disorder, social anxiety disorder, posttraumatic stress disorder and generalized anxiety disorder).

Mavoglurant (AFQ056) that is developed as a structurally novel, selective, noncompetitive antagonist for mGluR5 (Vranesic et al., 2014), has been investigated as an alternative treatment for FXS, OCD, PD-LID and Huntington's disease (Gomez-Mancilla et al., 2014; Reilmann et al., 2015; Rutrick et al., 2017). It binds to the same allosteric site on mGluR5 as [<sup>11</sup>C]-ABP688, a specific radioligand developed for positron emission tomography (PET) imaging of the mGlu5 receptor (Ametamey et al., 2006). Successful imaging of [<sup>11</sup>C]-ABP688 in the human brain has been demonstrated and brain kinetic data of [<sup>11</sup>C]-ABP688 readily fitted to a 2-tissue compartment model, suggesting specificity in binding (Ametamey et al., 2007; Treyer et al., 2008). In addition, the brain kinetic data were robust to noncompartmental modeling approaches such as Logan graphical analysis (Treyer et al., 2007).

The present study evaluates the relationship between brain mGlu5 receptor occupancy and the extent of plasma exposure following single oral doses of mavoglurant using [<sup>11</sup>C]-ABP688 PET imaging in healthy volunteers. mGlu5 receptor occupancy was also examined in various brain structures following single oral doses of mavoglurant. The study has helped to establish the binding of mavoglurant to the mGlu5 receptor in human brain in vivo, and the safety and tolerability of mavoglurant in healthy volunteers.

## 2. Methods

### 2.1. Study objectives

This study assessed the extent of mGlu5 receptor occupancy following single oral doses of mGluR5 antagonist, mavoglurant, in the striatum in healthy volunteers using [<sup>11</sup>C]-ABP688 PET imaging.

### 2.2. Study population

Six healthy male volunteers (aged 20–40 years) were enrolled in the study if they met the following eligibility criteria: male subjects in good health as determined by their past medical history, physical examination, vital signs, electrocardiogram (ECG) evaluation, and laboratory tests at the time of screening; vital signs within normal limits and no evidence of postural hypotension; body weight of at least 50 kg and a body mass index (BMI) in the range of 19–26 kg/m<sup>2</sup>; ability to provide written informed consent before the start of any study procedures; ability to communicate well with the investigator and comply with the requirements of the study.

All subjects enrolled in the study met the inclusion criteria at the screening visit and at baseline for all other treatment periods. At the time the study was conducted; we did not know whether subject characteristics (such as age and gender) might affect the distribution of the target or the pharmacokinetics of mavoglurant. We elected to restrict enrolment to healthy young adult males, to minimize potential between subject variability in a very small number of subjects.

### 2.3. Study design

This was an open-label, single-center pilot study conducted between 04 April 2006 and 28 September 2006 at the Psychiatric University Clinic, University of Zurich, Switzerland. Subjects were grouped into two cohorts (3 per cohort) and participated in a maximum 21-day screening period, three study periods (Periods 1, 2 and 3), followed by an overnight observation, with Periods 2 and 3 approximately one week apart. The three successive periods comprised a baseline [<sup>11</sup>C]-ABP688

PET scan (Period 1) and [<sup>11</sup>C]-ABP688 PET scans following two different single oral doses of mavoglurant (Periods 2 and 3). While subjects in cohort 1 received mavoglurant 25 mg and 200 mg doses, subjects in cohort 2 received mavoglurant 100 mg and 400 mg doses in Periods 2 and 3, respectively (Fig. 1A).

The final study protocol was approved by the Cantonal Ethics Committee of Canton Zurich and Swissmedic. This study was conducted in accordance with International Conference on Harmonization (ICH) Good Clinical Practice (GCP) regulations/guidelines, and in accordance with the ethical principles set forth in the Declaration of Helsinki. All subjects provided written informed consent before the study initiation.

#### 2.3.1. Preparation of [<sup>11</sup>C]-ABP688

The precursor ABG018 (corresponding unsubstituted oxime of ABP688) was prepared by Novartis Pharma AG, Basel. The radiotracer [<sup>11</sup>C]-ABP688 was prepared on site, at the PET Center of the University Hospital Zurich and the formulation for human application synthesized as described in Ametamey et al., 2007. The final production of [<sup>11</sup>C]-ABP688 was performed immediately before imaging due to the short half-life of <sup>11</sup>C (21 min).

#### 2.3.2. Procedures

Subjects who were admitted to the study center on the morning of Day 1, Period 1, and their eligibility confirmed based on inclusion and exclusion criteria and baseline clinical safety data, underwent a slow bolus i.v. injection of the tracer with 200 MBq (207±28.6 MBq, mean ±SD) [<sup>11</sup>C]-ABP688, including arterial and venous sampling (Fig. 1B). The choice of the [<sup>11</sup>C]-ABP688 dose was made based on the previously conducted validation studies and described by Ametamey et al., 2007, Treyer et al., 2007 and 2008 and to meet Swiss radiation dose limits in healthy subjects.

After an interval of 1–7 days, subjects received a single dose of 25 mg (cohort 1) or 100 mg (cohort 2) mavoglurant in Period 2, followed by a PET scan with [<sup>11</sup>C]-ABP688, 3 h post-drug administration, and with no arterial sampling. Subjects were observed for a minimum of 24 h post-drug administration and for another 72 h if clinically significant adverse events (AEs) were observed. A washout period of one week between Periods 2 and 3 was considered due to the half-life of 15 h for mavoglurant (Walles et al., 2013). A single dose of mavoglurant 200 mg (cohort 1) or 400 mg (cohort 2) was administered in Period 3 followed by a PET scan with [<sup>11</sup>C]-ABP688. Both arterial and venous sampling for plasma pharmacokinetics were measured in Period 3. Following each PET scan, subjects were observed for 24 h post-drug administration-dose (Fig. 1A). A study completion evaluation was conducted between 3 and 5 days after receiving the last oral dose and last [<sup>11</sup>C]-ABP688 PET scan.

#### 2.4. Imaging assessments

High resolution T1 images (1.5 Tesla scanner, GE Healthcare, at the Department of Medical Radiology of the Zurich University Hospital) were acquired for coregistration with PET scan image sets obtained on the Discovery-LS or Discovery-STRX PET camera (GE Healthcare) at Zurich University Hospital PET Center (camera of 55 cm gantry diameter, 144 mm axial field of view; image volumes consisted of 35 or 47 slices, 4.25 mm per slice; transmission scans were obtained using low-dose CT scan (140 kV, 40 mA). A clinical reading was also conducted to ensure that participants did not have evidence of significant neurological disease or pathology. All calculations were performed using the dedicated software PMOD (PMOD Technologies) (Mikolajczyk et al., 1998). Decay-corrected time-activity curves were generated for the following cerebral regions: anterior cingulate, medial temporal lobe, parietal cortex, cerebellum, and white matter. Values for the specific distribution volume (DV) were calculated from the estimated rate constants. MRI scans were superimposed on the emission data from [<sup>11</sup>C]-ABP688 PET scans and arterial input function were fit into compartmental (two-tissue

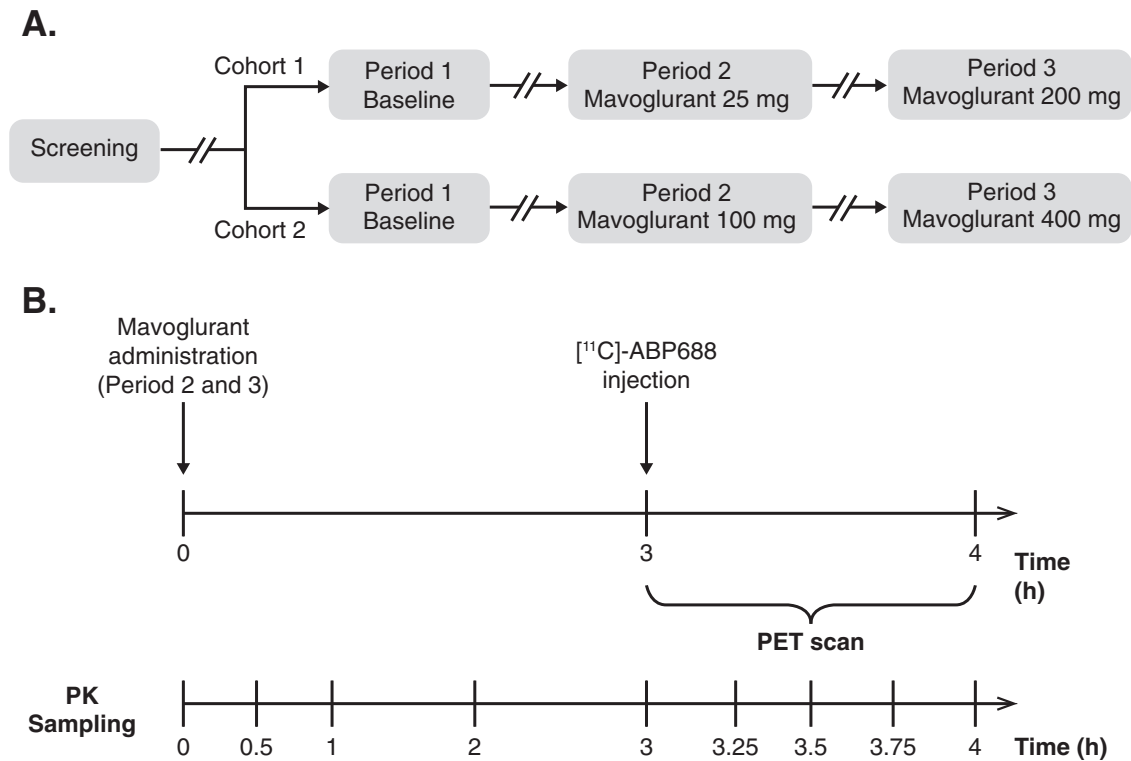


Fig. 1. A. Schematic representation of study design (whole period) B. Schematic representation of study design (single period).

compartment) and noncompartmental (with Logan analysis) models using PMOD to determine the model for best fit.

### 2.5. Drug concentrations

Mavoglurant concentrations in plasma were determined by a validated LC-MS/MS method, with a lower limit of quantification (LLOQ) of 2 ng/mL (Walles et al., 2013).

### 2.6. Data analysis

#### 2.6.1. Model implementation

mGlu5 receptor occupancy of single oral doses of mavoglurant was characterized by the  $EC_{50}$  (plasma concentration for 50% max relative displacement and 50% receptor occupancy) of the saturable binding model. Two-tissue and one-tissue compartment models were compared to determine the best fit. The brain kinetic data were readily fit to the two-compartment model as the optimal model, also suggesting specificity in binding and as demonstrated in Treyer et al., 2008. Best fit to  $[^{11}C]$ -ABP688 time-activity PET data was using arterial input function corrected for metabolites. The estimated rate constants of the model  $K_1$ ,  $k_2$ ,  $k_3$ ,  $k_4$  were used to estimate the binding potential relative to plasma ( $BP_p$ ) (Innis et al., 2007):

$$BP_p = \frac{K_1 k_3}{k_2 k_4} = f_p \frac{B_{avail}}{K_D}$$

$BP_p$  is the binding potential relative to plasma;  $f_p$  is the free fraction of tracer in plasma;  $B_{avail}$  is the available receptor density.

Displacement ( $D$ ) of  $[^{11}C]$ -ABP688 by mavoglurant was calculated as the percent reduction from baseline in  $BP_p$  measured during post-treatment PET scans (at scan time  $t$ ). This is proportional to the percentage change in receptor availability. Receptor occupancy (RO) of mGlu5 receptors by mavoglurant was inferred from the displacement via a saturation binding equation, as described below.

$$D = 1 - BP_p(treatment)/BP_p(baseline)$$

$D$  is the displacement;  $BP_p$  is the binding potential relative to plasma

#### 2.6.2. Displacement versus plasma concentration

The relationship between mavoglurant plasma concentrations and relative displacement of  $[^{11}C]$ -ABP688 was investigated graphically. An exploratory analysis was conducted to estimate the plasma concentration associated with 50% displacement through the  $E_{max}$  model:

$$D = \frac{E_{max} * C_p}{EC_{50} + C_p}$$

$D$  is the displacement;  $C_p$  is the plasma concentration of mavoglurant at time  $t$ ;  $E_{max}$  is the maximum attainable displacement at very high plasma concentrations;  $EC_{50}$  is the plasma concentration that yields 50% of maximum relative displacement

#### 2.6.3. Displacement versus dose

In parallel to the above concentration-response analysis, a dose-response analysis was also conducted to estimate the dose associated with 50% displacement (at scan time) through the following saturation displacement formula:

$$D = \frac{E_{max} * Dose}{ED_{50} + Dose}$$

$D$  is the displacement; dose is the dose of mavoglurant;  $E_{max}$  is the maximum attainable displacement at scan time 3–4 h post-dose at very high doses;  $ED_{50}$  is the dose that yields 50% of maximum relative displacement at scan time of 3–4 h post-dose.

#### 2.6.4. Receptor occupancy

Receptor occupancy versus plasma concentration:

Even if the receptor occupancy of mGlu5 is not directly observed, assuming that 100% receptor occupancy corresponds to the maximum displacement, then the following can be inferred:

$$RO = \frac{C_p}{EC_{50} + C_p}$$

**Table 1**

Mavoglurant pharmacokinetics after single administration of 25 mg, 100 mg, 200 mg and 400 mg in healthy volunteers.

Parameter	Mavoglurant 25 mg	Mavoglurant 100 mg	Mavoglurant 200 mg	Mavoglurant 400 mg
N	5	3	4	3
$t_{\max}$ (h)	2.00 (2.00–3.25)	3.25 (2.00–3.50)	2.50 (1.00–4.02)	2.00 (2.00–3.00)
$C_{\max}$ (ng/mL)	54.23 ± 39.09 (39.3)	191.6 ± 112.5 (160.0)	337.6 ± 217.6 (267.0)	1004 ± 674.1 (837.2)
$AUC_{3-4}$ (ng.h/mL)	31.42 ± 17.84 (25.30)	156.3 ± 103.7 (130.0)	202.8 ± 99.35 (177.4)	715.0 ± 429 (597.7)
$AUC_{0-12}$ (ng.h/mL)	200.9 ± 107.6 (169.3)	957.5 ± 524.8 (823.5)	1798 ± 946.0 (1492)	5054 ± 3409 (4156)
$AUC_{0-24}$ (ng.h/mL)	253.3 ± 143.3 (211.5)	1221 ± 628.5 (1075)	2396 ± 1210 (1998)	6939 ± 4946 (5587)

$t_{\max}$  values presented as median (range);  $C_{\max}$ ,  $AUC_{0-1}$ ,  $AUC_{0-12}$  and  $AUC_{0-24}$  values represented as mean ± SD (geometric mean).

Half-life of mavoglurant is estimated to be around 15 h based on previous studies (Walles et al., 2013).

RO is the receptor occupancy of mGluR5 by mavoglurant;  $C_p$  is the plasma concentration of mavoglurant;  $EC_{50}$  is again the plasma concentration observed to yield 50% of maximum relative displacement; assumed to yield 50% RO.

### 2.6.5. Receptor occupancy through the dose-response analysis

Similarly, for the dose-response analysis, we infer receptor occupancy at scan time of 3–4 h post-dose as below:

$$RO = \frac{Dose}{ED_{50} + Dose}$$

RO is the receptor occupancy of mGluR5 by mavoglurant; dose is the dose of mavoglurant;  $ED_{50}$  is again the dose that yields 50% of maximum relative displacement at scan time of 3–4 h post-dose, assumed to yield 50% RO.

### 2.7. Statistical methods

No sample size calculations were performed as this was a pilot exploratory study with only three participants per dose group. Values of RO were provided by brain region relative to baseline per subject and listed together with the plasma PK parameters for each parameter derived from PET scans. The data were presented descriptively and no formal statistical comparisons were made. The relationship between exposure and occupancy at other brain regions and between mavoglurant plasma concentrations with the mGlu5 receptor occupancy was presented graphically.

## 3. Results

### 3.1. Subject disposition and demographics

A total of six subjects were enrolled in the study. Two of the six participants chose to discontinue the study for personal reasons following technical problems with the ABP688 bolus injection (synthesis failure). These participants were replaced by another two subjects, both of whom completed the study. All eight participants enrolled were men, Caucasian, with mean (SD) age 27.4 (6.25) years and mean BMI 23.25 (1.6) kg/m<sup>2</sup>.

### 3.2. Pharmacokinetic assessments

After administration of a single dose in healthy participants, mean  $C_{\max}$  and AUC values increased with dose (Table 1). Onset of mavoglurant absorption was fast and no lag time was observed. Maximum concentrations of mavoglurant were observed around 2–3.25 h post-dose.

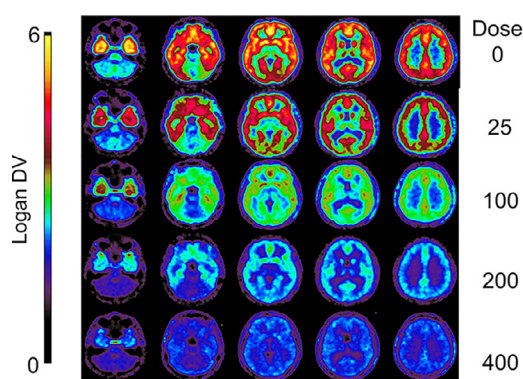


**Fig. 2.** Representative DV Logan images showing the effect of mavoglurant on binding of [<sup>11</sup>C]-APB688. Normalized and averaged DV Logan images for each dose cohort visualize the distribution and uptake values on axial slices from cerebellum to cortical regions. Logan Plot method was chosen for the pixel wise modeling for improved image quality. DV, distribution volume.

### 3.4. Analysis of receptor occupancy

The highest distribution volume ( $BP_p$ ) of ABP688 was observed in the anterior cingulate region whereas the white matter and cerebellum showed a low uptake (Table 2, Fig. 2). The distribution volumes ( $BP_p$ ) were in line with previously published data using ABP688 (Ametamey et al., 2007) across regions. The  $E_{\max}$  model was the best fit to each individual region of the brain (estimates ranging from 56% to 72%) except to the cerebellum and white matter (outlying low  $E_{\max}$  estimates of 35% and 27%); these regions were not used in the analysis of pooled cortical areas. The displacement measured was regressed on doses and on plasma concentrations between 3 and 4 h after drug intake (time of the PET scan).

$RO_{50}$  and  $E_{\max}$  based on plasma concentrations for each individual region of the brain, and for the pooled displacement across all regions (except cerebellum and white matter), are presented in Table 3.

The pooled displacement values for each individual (summing across all regions except cerebellum and white matter) were plotted versus plasma concentration using a linear concentration scale (Fig. 3A) and a logarithmic concentration scale (Fig. 3B). Assuming that the  $E_{\max}$  corresponds to mGlu5 receptor occupancy of 100% and therefore, the observed  $EC_{50}$  is the same for the receptor occupancy, the prediction curve of the RO was plotted versus the plasma concentration (Fig. 4A) and the dose between 3 and 4 h (Fig. 4B).

The  $RO_{50}$  of striatum (caudate and putamen) did not differ from other regions of the cerebral cortex. The  $E_{\max}$  was also similar across

**Table 2**  
Distribution volume ( $BP_p$ ) and ratio  $k_3/k_4$  ( $BP_{ND}$ ) per region at baseline.

Region	Distribution volume ( $BP_p$ )	Ratio $K3/K4$ ( $BP_{ND}$ )
Anterior cingulum	5.28 (1.08)	7.1 (2.09)
Caudate	4.99 (1.18)	7.02 (2.46)
Cerebellum	2.01 (0.36)	2.72 (0.86)
Frontal cortex	4.5 (1.04)	5.91 (2.05)
Lateral temporal cortex	4.52 (1.07)	6.05 (1.92)
Medial orbitofrontal cortex	5.24 (1.11)	7.13 (2.33)
Mediotemporal cortex (mainly hippocampus)	5.05 (1.51)	6.62 (2.18)
Occipitotemporal cortex	4.09 (1.07)	5.53 (1.8)
Orbitofrontal cortex	4.39 (1.06)	5.96 (2.06)
Parietal cortex	4.11 (0.84)	5.57 (1.82)
Posterior cingulum	4.65 (0.96)	6.39 (2.13)
Prefrontal cortex	4.19 (0.91)	5.53 (1.74)
Putamen	4.75 (1.03)	6.55 (1.93)
Thalamus	3.34 (0.62)	4.4 (1.27)
Ventral part of anterior cingulum	5.52 (1.23)	7.43 (2.46)
Visual cortex	3.77 (0.92)	5.12 (1.87)
White matter	1.8 (0.45)	2.44 (0.89)
Mean across all regions except cerebellum and white matter	5.28 (1.08)	7.1 (2.09)

Data are expressed as mean (SD).

$BP_{ND}$ , binding potential relative to the nondisplaceable compartment.

$BP_p$  refers to the ratio at equilibrium of specifically bound radioligand to that of total parent radioligand in plasma (i.e., free plus protein bound, excluding radioactive metabolites).

$BP_{ND}$  refers to the ratio at equilibrium of specifically bound radioligand to that of nondisplaceable radioligand in tissue.

**Table 3**  
Estimated  $EC_{50}$  and  $ED_{50}$  per region of the brain.

Region	Estimated $ED_{50}$	Std. Error	Estimated $EC_{50}$	Std. Error
Anterior cingulum	65	18	43	14
Caudate	77	21	58	20
Cerebellum	53	53	33	33
Frontal cortex	61	18	38	15
Lateral temporal cortex	66	13	35	13
Medial orbitofrontal cortex	64	16	42	14
Mediotemporal cortex (mainly hippo)	69	18	38	17
Occipitotemporal cortex	69	22	43	18
Orbitofrontal cortex	71	22	36	16
Parietal cortex	68	21	39	16
Posterior cingulum	62	23	44	17
Prefrontal cortex	76	21	45	17
Putamen	68	21	50	16
Thalamus	72	20	38	14
Ventral part of anterior cingulum	80	23	50	18
Visual cortex	65	27	46	21
White matter	139	175	9	19
Mean across all regions except cerebellum and white matter	69	24	43	20

$EC_{50}$  is the plasma concentration (ng/mL) and  $ED_{50}$  the dose which corresponds to 50% receptor occupancy.

the cortical regions and striatum. Low  $E_{max}$  observed in the cerebellum and white matter is in line with receptor distribution in humans lacking expression in these regions. The observed  $E_{max}$  in 'target' regions (other than the white matter and cerebellum) was 65%. This suggests that there is still specific binding of [ $^{11}C$ ]-ABP688 at high concentrations of mavoglurant. Estimated receptor occupancy (% occupancy) at 3–4 h post-dose was 27% (mavoglurant 25 mg), 59% (mavoglurant 100 mg), 74% (mavoglurant 200 mg), and 85% (mavoglurant 400 mg) (Fig. 3A).

Across all regions except cerebellum and white matter, the observed  $EC_{50}$  for AFQ056 at the mGlu5 receptor was 43 (+/- 20) ng/mL (Table 3). A similar evaluation, regressing the displacement versus the dose delivered an  $ED_{50}$  of 69 mg (Table 3).

#### 4. Discussion

The use of PET scanning with [ $^{11}C$ ]-ABP688 has proved to be an important tool to study expression of altered mGlu5 receptors in various developmental, psychiatric, neurodegenerative, and neurological disorders (Kim et al., 2019; Mihov et al., 2020; Smart et al., 2020). Inte-

grating the use of PET imaging with [ $^{11}C$ ]-ABP688 to the determination of the relationship between receptor occupancy and the dose/blood exposure has the potential to optimize the dose finding and/or determine specific binding to mGlu5 receptors of noncompetitive antagonists of the mGlu5 receptor in humans and non-human primates (Kagedal et al., 2013; Mathews et al., 2014).

Mavoglurant was developed as a structurally novel, subtype selective, noncompetitive antagonist at the mGlu5 receptor. It exhibits clear anxiolytic actions in a variety of animal models, suggesting the potential to treat various anxiety disorders including panic disorder, social anxiety disorder, posttraumatic stress disorder and generalized anxiety disorder. The results of the present study and the human PK profile of mavoglurant (Walles et al., 2013) were key to guide the choice of dose and regimen used in the clinical trials conducted with mavoglurant. Lack of efficacy reported in obsessive compulsive disorders (Rutrick et al., 2017). Although, the dosing and regimen used in the Huntington's disease (Reilmann et al., 2015), the obsessive compulsive disorders (Rutrick et al., 2017) and Fragile X (adults and adolescents) studies was such that it resulted in 80% receptor occupancy, this did not result in

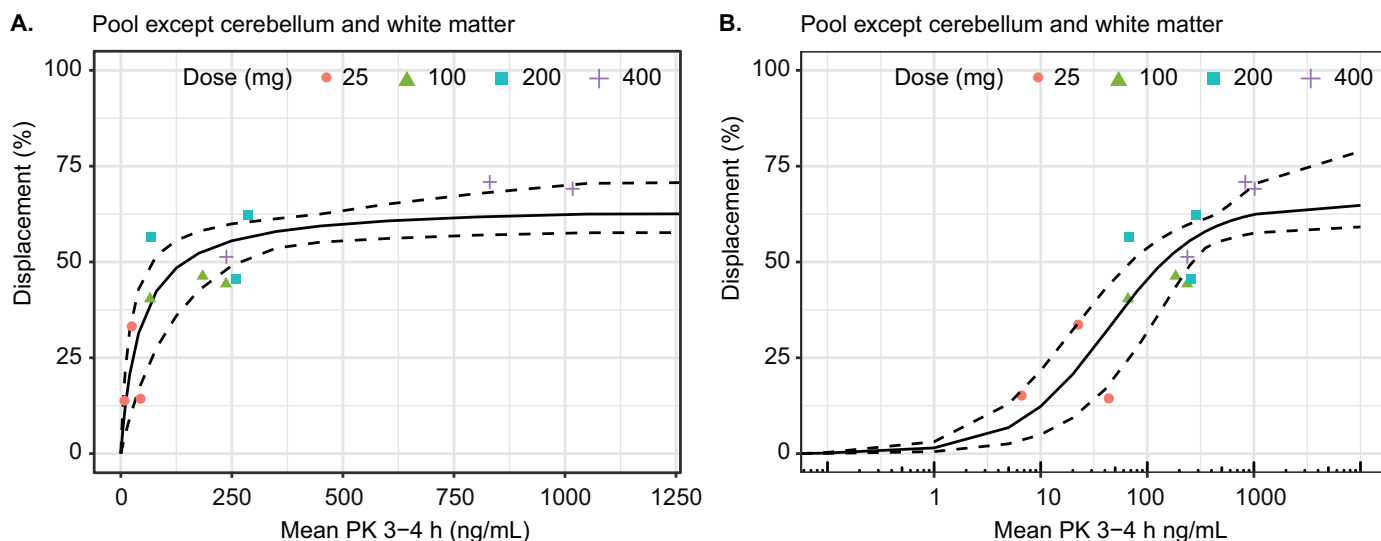


**Fig. 3.** Displacement vs blood concentrations  
Relative displacement versus blood concentrations (ng/mL) at 3–4 h post dose. **A.** Linear concentration scale **B.** Logarithmic concentration scale. Data comprised pooled displacement values summing across all regions except cerebellum and white matter.

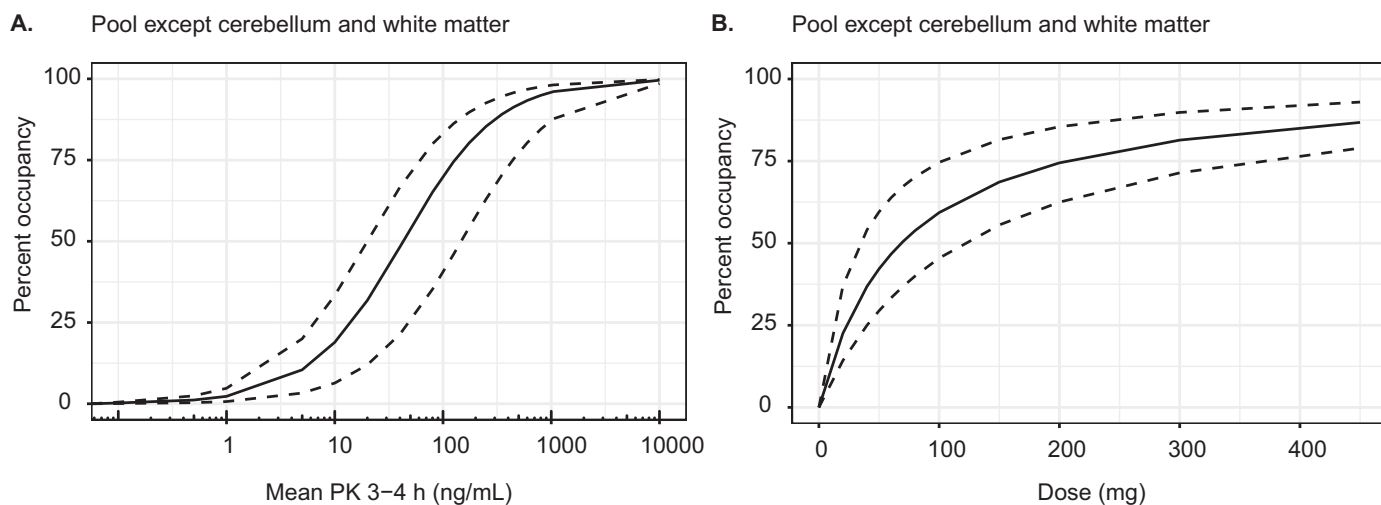


**Fig. 4.** Estimated receptor occupancy versus dose and blood concentration  
**A.** Estimated receptor occupancy versus blood concentrations (ng/mL) **B.** Estimated receptor occupancy at 3–4 h post dose versus dose.

efficacy during the treatment period. Similarly for FXS, another selective mGluR5 antagonist (basimglurant) did not achieve efficacy while achieving sufficient receptor occupancy (Quiroz et al., 2016). Taken together, these results indicate that mGluR5 antagonists might not be a therapeutic option for these pathologies.

The situation appears to be different in Parkinson’s disease where mavoglurant demonstrated efficacy in reducing L-Dopa induced dyskinesia in two proof of principle trials (150 mg b.i.d.; Berg et al., 2011) and at the highest dose (100 mg b.i.d.) in a phase IIb trial; Stocchi et al., 2013). In contrast, no efficacy could be demonstrated in other trials (100, 150, 200 mg b.i.d.; Trenkwalder et al., 2016).

Mavoglurant binds to all mGlu5 receptors in brain regions of interest. Mavoglurant passes the blood–brain barrier and induces a dose/exposure-dependent displacement of [<sup>11</sup>C]-ABP688 bound to mGlu5 receptors in humans in vivo. The study procedures for safety and blood sampling were well tolerated with no serious AEs or dropouts due to AEs. PET and [<sup>11</sup>C]-ABP688 provide a unique tool to study drug-induced occupancy of mGlu5 receptors in the brain.

The distribution volumes of mavoglurant agree well with previously published data, with the highest distribution volumes observed in the cingulate region (Ametamey et al., 2007). Relatively lower uptake is observed in the nontarget regions, cerebellum and white matter, possibly due to the presence of myelinated axonal sheets that are likely devoid of mGlu5 receptors and sheathed from drug absorption. Mavoglurant binds to mGluR5 receptor thus blocking [<sup>11</sup>C]-ABP688 from cortical receptor regions of interest. A single oral dose of 400 mg induced an estimated displacement of 63% at scan time of 3–4 h post-dose, inferring a receptor occupancy estimate of nearly 85%.

Despite many studies involving the mGlu5 receptor in various disorders, this receptor and its interactions are yet to be fully understood before its application as a therapeutic target.

### 5. Conclusion

The results of this study clearly demonstrate that Mavoglurant penetrates the brain and dose/exposure dependently prevents the binding



of [<sup>11</sup>C]-ABP688 from the mGlu5 receptors in humans in vivo. In addition, mavoglurant binds evenly to all mGlu5 receptor brain regions of interest. The results of this study have been of key importance in determining the clinical doses of mavoglurant in the conducted clinical trials. The study shows that [<sup>11</sup>C]-ABP688 PET imaging provides a unique tool to study drug-induced occupancy of mGlu5 receptors in the living human brain.

### Declaration of Competing Interest

JS, VT, AB, SA, MB, RPM have no conflict of interest; MES holds Novartis shares; AG, YPA, I-TV, BG-M, FG are employees of Novartis.

### CRedit authorship contribution statement

**Johannes Streffer:** Conceptualization, Methodology, Project administration, Formal analysis, Visualization, Writing – Review & Editing. **Valerie Treyer:** Methodology, Project administration, Formal analysis, Writing – Review & Editing. **Alfred Buck:** Methodology, Validation, Formal analysis. **Simon Ametamey:** Project administration, Formal analysis, Supervision, Writing – Review & Editing. **Milen Blagoev:** Project administration, Writing – Review & Editing, Involvement in radiosynthesis of [<sup>11</sup>C]-ABP688. **Ralph P Maguire:** Formal analysis, Supervision, Writing – Review & Editing, Author of the original Novartis study report upon which the manuscript is based. **Aurélié Gautier:** Formal analysis, Data curation, Writing – Review & Editing. **Yves P. Auberson:** Writing – Review & Editing, Involvement in [<sup>11</sup>C]-ABP688 development and use as a receptor occupancy tracer. **Mark E. Schmidt:** Conceptualization, Methodology, Writing – Review & Editing. **Ivan-Toma Vranesic:** Conceptualization, Formal analysis, Data curation, Writing – Review & Editing, Involvement with ABP688 and AFQ056 projects, leader on preclinical activities with ABP688 at the time of the study. **Baltazar Gomez-Mancilla:** Conceptualization, Methodology, Project administration, Formal analysis, Data curation, Supervision, Funding acquisition, Resources, Writing – Review & Editing. **Fabrizio Gasparini:** Conceptualization, Methodology, Project administration, Supervision, Funding acquisition, Resources, Writing – Review & Editing.

### Acknowledgments

This study was funded by Novartis Pharma AG, and the precursor ABG018 (corresponding unsubstituted oxime of ABP688) was prepared by them. The authors acknowledge the patients, investigators and staff at participating sites for supporting the conduct of the study. All named authors meet the International Committee of Medical Journal Editors (ICMJE) criteria for authorship for this manuscript, take responsibility for the integrity of the work as a whole. All authors are responsible for intellectual content and data accuracy. We thank Suchitra Jagannathan and Shyamashree Dasgupta (Novartis Healthcare Pvt. Ltd., Hyderabad, India) for providing medical writing support. All authors had full access to all data in the study and had final responsibility for the decision to submit for publication.

### Data code and availability statement

Data is not openly available due to privacy issues of clinical data.

### References

- Akkus, F., et al., 2014. Metabotropic glutamate receptor 5 binding in patients with obsessive-compulsive disorder. *Int. J. Neuropsychopharmacol.* 17, 1915–1922.
- Ametamey, S.M., et al., 2006. Radiosynthesis and preclinical evaluation of [<sup>11</sup>C]-ABP688 as a probe for imaging the metabotropic glutamate receptor subtype 5. *J. Nucl. Med.* 47, 698–705.
- Ametamey, S.M., et al., 2007. Human PET studies of metabotropic glutamate receptor subtype 5 with [<sup>11</sup>C]-ABP688. *J. Nucl. Med.* 48, 247–252.
- Berg, D., et al., 2011. AFQ056 treatment of levodopa-induced dyskinesias: results of 2 randomized controlled trials. *Mov. Disord.* 26, 1243–1250.
- Dolen, G., Bear, M.F., 2008. Role for metabotropic glutamate receptor 5 (mGluR5) in the pathogenesis of fragile X syndrome. *J. Physiol.* 586, 1503–1508.
- Gomez-Mancilla, B., et al., 2014. Development of mavoglurant and its potential for the treatment of fragile X syndrome. *Expert Opin. Investig. Drugs* 23, 125–134.
- Innis, R.B., et al., 2007. Consensus nomenclature for in vivo imaging of reversibly binding radioligands. *J. Cereb. Blood Flow Metab.* 27, 1533–1539.
- Jaeschke, G., et al., 2015. Metabotropic glutamate receptor 5 negative allosteric modulators: discovery of 2-chloro-4-[1-(4-fluorophenyl)-2,5-dimethyl-1H-imidazol-4-ylethynyl]pyridine (basimglurant, RO4917523), a promising novel medicine for psychiatric diseases. *J. Med. Chem.* 58, 1358–1371.
- Kagedal, M., et al., 2013. A positron emission tomography study in healthy volunteers to estimate mGluR5 receptor occupancy of AZD2066 - estimating occupancy in the absence of a reference region. *Neuroimage* 82, 160–169.
- Kim, J.-H., et al., 2019. In vivo metabotropic glutamate receptor 5 availability-associated functional connectivity alterations in drug-naïve young adults with major depression. *Eur. Neuropsychopharmacol.* 29, 278–290.
- Mathews, W.B., et al., 2014. Dose-dependent, saturable occupancy of the metabotropic glutamate subtype 5 receptor by fenobam as measured with [(11) C]ABP688 PET imaging. *Synapse* 68, 565–573.
- Michalon, A., et al., 2012. Chronic pharmacological mGlu5 inhibition corrects fragile X in adult mice. *Neuron* 74, 49–56.
- Mihov, Y., et al., 2020. Metabotropic glutamate receptor 5 in bulimia nervosa. *Sci. Rep.* 10, 6374.
- Mikolajczyk, K., et al., 1998. A JAVA environment for medical image data analysis: initial application for brain PET quantitation. *Med. Inform. (Lond.)* 23, 207–214.
- Quiroz, J.A., et al., 2016. Efficacy and safety of basimglurant as adjunctive therapy for major depression: a randomized clinical trial. *JAMA Psychiatry* 73, 675–684.
- Reilmann, R., et al., 2015. A randomized, placebo-controlled trial of AFQ056 for the treatment of chorea in Huntington's disease. *Mov. Disord.* 30, 427–431.
- Reiner, A., Levitz, J., 2018. Glutamatergic signaling in the central nervous system: ionotropic and metabotropic receptors in concert. *Neuron* 98, 1080–1098.
- Rutrick, D., et al., 2017. Mavoglurant augmentation in OCD patients resistant to selective serotonin reuptake inhibitors: a proof-of-concept, randomized, placebo-controlled, phase 2 study. *Adv. Ther.* 34, 524–541.
- Smart, K., et al., 2020. Metabotropic glutamate type 5 receptor binding availability during dextroamphetamine sensitization in mice and humans. *J. Psychiatry Neurosci.* 45 (4), 190162. doi:10.1503/jpn.190162, Online ahead of print.
- Stocchi, F., et al., 2013. AFQ056 in Parkinson patients with levodopa-induced dyskinesias: 13-week, randomized, dose-finding study. *Mov. Disord.* 28, 1838–1846.
- Suh, Y.H., et al., 2018. Metabotropic glutamate receptor trafficking. *Mol. Cell Neurosci.* 91, 10–24.
- Swanson, C.J., et al., 2005. Metabotropic glutamate receptors as novel targets for anxiety and stress disorders. *Nat. Rev. Drug Discov.* 4, 131–144.
- Trenkwalder, C., et al., 2016. Mavoglurant in Parkinson's patients with L-Dopa-induced dyskinesias: two randomized phase 2 studies. *Mov. Disord.* 31, 1054–1058.
- Treyer, V., et al., 2007. Evaluation of the metabotropic glutamate receptor subtype 5 using PET and [<sup>11</sup>C]-ABP688: assessment of methods. *J. Nucl. Med.* 48, 1207–1215.
- Treyer, V., et al., 2008. Radiation dosimetry and biodistribution of [<sup>11</sup>C]-ABP688 measured in healthy volunteers. *Eur. J. Nucl. Med. Mol. Imaging* 35, 766–770.
- Vose, L.R., Stanton, P.K., 2017. Synaptic plasticity, metaplasticity and depression. *Curr. Neuropharmacol.* 15, 71–86.
- Vranesic, I., et al., 2014. AFQ056/mavoglurant, a novel clinically effective mGluR5 antagonist: identification, SAR and pharmacological characterization. *Bioorg. Med. Chem.* 22, 5790–5803.
- Wallis, M., et al., 2013. Metabolism and disposition of the metabotropic glutamate receptor 5 antagonist (mGluR5) mavoglurant (AFQ056) in healthy subjects. *Drug Metab. Dispos.* 41, 1626–1641.